Am J Transl Res 2021;13(9):10896-10907
www.ajtr.org /ISSN:1943-8141/AJTR0134428

Original Article

LncRNA GAS5 enhances radiosensitivity of hepatocellular carcinoma and restricts tumor growth and metastasis by miR-144-5p/ATF2

Chuanyun Yu[1*], Yi Liang[1], Yiqiang Jin[2*], Qinghuan Li[1]

[1]Oncology Radiotherapy Center, Xiangyang Central Hospital, Affiliated Hospital of Hubei University of Arts and Science, Xiangyang 441021, Hubei, China; [2]Department of Oncology, Xiangyang Central Hospital, Affiliated Hospital of Hubei University of Arts and Science, Xiangyang 441021, Hubei, China. [*]Equal contributors.

Received April 18, 2021; Accepted July 28, 2021; Epub September 15, 2021; Published September 30, 2021

Abstract: Background: This study aimed to evaluate the biologic role of growth arrest-specific 5 (GAS5) in radiosensitivity of hepatocellular carcinoma (HCC). Methods: The levels of GAS5, miR-144-5p, and activating transcription factor 2 (ATF2) were quantified in HCC tissues and cell lines. RNA immunoprecipitation (RIP) and RNA pull-down assays were used to test the interaction between GAS5 and miR-144-5p. The regulatory relationship between miR-144-5p and ATF2 was identified by the dual-luciferase reporter (DLR) assay. A nude mouse model of HCC was induced to verify the effect of GAS5 on radiosensitivity of HCC *in vivo*. Results: Lower levels of GAS5 and ATF2, and higher levels of miR-144-5p, were found in radiation-resistant human HCC tissues and cell lines. Overexpression of ATF2 or GAS5 enhanced the radiosensitivity of HCC cell lines, while knockdown of ATF2 or GAS5 decreased the radiosensitivity. In addition, GAS5 acted as a miR-144-5p sponge, and miR-144-5p inversely regulated ATF2. Also, GAS5 mediated ATF2 levels through miR-144-5p, and increased the radiosensitivity of HCC by suppressing miR-144-5p both *in vivo* and *in vitro*. Conclusion: Overexpression of GAS5 upregulates ATF2 through miR-144-5p and is able to enhance the radiosensitivity of HCC.

Keywords: Hepatocellular carcinoma, GAS5, ATF2, miR-144-5p, radiotherapy

Introduction

Changes in eating habits and the environment may contribute to an increasing incidence of cancers. Hepatocellular carcinoma (HCC) is a major malignancy with the highest incidence worldwide [1]. More than 800,000 new cases and 780,000 deaths are reported globally every year, with a ratio of deaths to new cases of approximately 1:1.07 [2]. In addition, with the continuous advances in diagnostic techniques and the popularization of tumor screening, the incidence of HCC has been increasing in younger people [3, 4]. There are multiple pathogenic factors of HCC, among which obesity, diabetes, alcohol consumption and persistent hepatitis B or C virus infection are the most common [5, 6]. Surgery is the first choice for the treatment of HCC, but not all patients have this opportunity. Because of metastasis of advanced cancers, patients can improve their condition only through radiotherapy [7]. Radiotherapy has played a key role in a variety of malignancies [8]. It is reported that radiosensitivity of tumor cells is related to cell vitality, cell cycle distribution, DNA damage repair and apoptosis [9]. However, long-term radiotherapy is likely to induce radiation resistance, thereby leading to a decline in clinical efficacy and even treatment failure [10]. Therefore, it is imperative to enhance the radiosensitivity of HCC so as to improve the curative effect.

Long-chain non-coding RNAs (lncRNAs), transcription factors with a length of over 200 nucleotides, have been considered to be waste products because of their lack of protein coding ability [11]. However, an imbalance of lncRNAs has been recently found to relate to tumor progression [12]. Moreover, there is evidence that lncRNAs also may act as competitive endogenous RNAs (ceRNAs) [13]. Rui et al. have indi-

cated that inhibiting lncRNA PCAT6 increases the radiosensitivity of triple negative breast cancer (TNBC) cells through the miR-185-5p/TPD52 axis [14]. The lncRNA growth arrest-specific 5 (GAS5), also known as SNHG2, is an early discovered lncRNA located at human 1q25.1 [15]. GAS5 has the function of regulating the domain of glucocorticoid receptors [16], which means that the transcription of GAS5 is able to induce apoptosis. Additionally, Zhao et al. have proposed that GAS5 can increase the sensitivity of HCC to CDDP by sponging miR-222 [17]. Nevertheless, there is no study showing that GAS5 can increase the radiosensitivity of HCC.

Therefore, the present study is designed to evaluate the regulatory role of GAS5 in the radiosensitivity of HCC, aiming to offer an available target to the clinic.

Methods and data

Clinical data of patients

Forty pairs of HCC tissue and adjacent tissue samples collected from patients admitted from May, 2013 to May, 2014 were collected for this study. All patients had received anti-tumor therapy (surgery, chemotherapy and radiotherapy), and had signed informed consent. Ethics approval was granted by hospital Medical Committee (XY2012ZX09102), and this study was in accordance with the Declaration of Helsinki [18].

Cell culture

HCC cell lines (Hep3B, SK-HEP-1) and human liver cell line (THLE-2) (ATCC, Manassas, VA, USA) were grown in DMEM (Gibco) supplemented with 10% FBS at 37°C and 5% CO_2. Hep3B and SK-HEP-1 cells ($5*10^3$) were separately irradiated by a 6-MV linear accelerator at the doses of 0, 2, 4, 6 and 8 Gy. After radiation for 24 hours, the cells were collected. Those irradiated at a dose of 6 Gy were examined every 6 hours until radiation for 24 hours.

Cell transfection

pcDNA3.1-GAS5 (negative control: pcDNA-3.1-NC) was synthesized with pcDNA3.1 as vector. In addition, small interfering RNA (siRNA), si-GAS5#1, Si-GAS5#2 and Si-GAS5#3, as well as si-ATF2 and si-NC were also constructed. The miR-144-5p mimetic, NC-mimetic, ATF2 overexpression vector (pcDNA-3.1-ATF2), blank overexpression vector (vector), miR-144-5p inhibitor (anti-mi-miR-144-5p) and anti-miR-NC (all from RiboBio, Guangzhou, China) were synthesized. These plasmids and oligonucleotides were transfected into HCC cells using Lipofectamine 3000 (Carlsbad, California, USA). Overexpression plasmid transfection: The serum-free medium (250 μL) was used to dilute the transfection reagent Lipofectamine 3000 (12.5 μL). Then, the overexpression plasmid (4.2 μg) and P3000 (8 μL) were added into serum-free culture medium (250 μL), which were mixed respectively and incubated at room temperature for 5 min. Finally, the solution was mixed and incubated at room temperature for 15 min. Transfection of siRNA and miR: The serum-free medium (250 μL) was used to dilute the transfection reagent Lipofectamine 3000 (12.5 μL) (solution A). The siRNA or miR (12.5 μL) were added into serum-free culture medium (250 μL) to adjust the final concentration of siRNA or miR to 50 nM. Then, they were mixed respectively and incubated at room temperature for 5 min. Then, the liquids were mixed evenly and incubated at room temperature for 15 min.

qRT-PCR

Reverse transcription of RNA extracted from samples with Trizol reagent (Invitrogen) was performed with Reverse EasyScript One-Step gDNA Removal and cDNA Synthesis SuperMix (Trangene, Beijing, China). PCR amplification was conducted on an Applied Biosystems 7500 (ABI, USA) with SYBR Premix Ex Taq II (TaKaRa, Dalian, China). Relative levels of GAS5, miR-144-5p, and ATF2 were quantified by $2^{-\Delta\Delta Ct}$, and GAPDH and U6 served as internal references [19]. The upstream primer of GAS5 was 5'-CTTCTGGGCTCAAGTGATCCT-3', and the downstream primer was 5'-TTGTGCCATGAGACTCCATCAG-3'. The upstream primer of miR-144-5p was 5'-CGGGCGATATCATCATATACTG-3', and the downstream primer was 5'-GTGCAGGGTCCGAGGT-3'. The upstream primer of ATF2 was 5'-CAATCCACTGCCATGGCCTT-3', and the downstream primer was 5'-TCAGATAAAGCCAAGTCGAATCTGG-3'. The upstream primer of GPADH was 5'-GTCAACGGATTTGGTCTGTATT-3', and the downstream primer was 5'-AGTCTTCTGGGTGGCAGTGAT-3'. The upstream primer of U6 was 5'-CTCGCTTCGG-

CAGCACA-3', and the downstream primer was 5'-AACGCTTCACGAATTTGCGT-3'.

Colony survival assay

The transfected cells were collected into a 6-well plate for a 48-h incubation. Next, the cells were irradiated at a dose rate of 400 cGy/min (0, 2, 4, 6 and 8 gy). After that, the cells were inoculated in a 60 mm Petri dish at 37°C until cell colonies were visible, and then stained with 1% crystal violet, and counted under a microscope. Cell survival was calculated.

Cell proliferation assay

3-(4,5-dimethyl-2-thiazolyl)-2,5-diphenyl-2-H-tetrazole bromide (MTT, Solarbio, Beijing, China) was used to measure cell proliferation. The cells at a concentration of 2.0×10^3 cells/mL were grown in a 96-well plate. After incubation for 24 hours, MTT solution was added to each well. Cells were treated with DMSO (Solarbio) for 15 minutes at the 24th, 48th, 72nd and 96th hours, and cell proliferation was tested at 490 nm using a microplate reader (Thermo Fisher Scientific, USA).

Cell apoptosis assay

FITC/PI staining was conducted for apoptosis measurement. Transfected cells were subjected to 6-Gy radiation for 24 hours, and those without ionizing radiation treatment served as controls. Annexin V-FITC (10 μL, K201-100, Biovision, Mountain View, CA, USA) and PI (5 μL) were added, mixed and reacted in the dark for 15 minutes. Following the addition of binding buffer (300 μL), cell apoptosis was tested by flow cytometry at the excitation wavelength of 488 nm.

Western blot (WB)

Total protein was extracted from transfected cells by RIPA buffer (Invitrogen), and then separated by SDS-PAGE and blotted to a PVDF membrane (Bio-Rad, Inc., CA, USA). After blocking with skim milk for 1 hour, the membrane was incubated with rabbit anti-human primary antibodies against Bcl-2 (1:1000, ab32124, Abcam Inc, USA), Bax (1:1000, ab32503, Abcam Inc, USA), cle-caspase-3 (1:500, ab13847, Abcam Inc, USA), ATF2 (1:500, ab239361, Abcam Inc, USA) and GAPDH (1:5000, ab8245, Abcam Inc, USA) overnight at 4°C. Following 3 TBST washes, goat anti-rabbit secondary antibody (HRP) was added, incubated for 1 hour. Next, the membrane was developed by enhanced chemiluminescence. Images were scanned, and gray values of bands were analyzed by a gel imaging system (Bio-Rad iQ5, Bio-Rad, Inc., CA, USA).

Dual-luciferase reporter (DLR) assay

Binding sites of miR-144-5p were predicted online by LncBase [20] and starBase 3.0 [21]. HCC cells were co-transfected with GAS5-WT/MUT or ATF2 3'UTR-WT/MUT and miR-144-5p mimics or NC miRNA (NC-mimics) for 48 hours. Luciferase activity was visualized in a DLR assay system (Promega Corporation, Madison, Wisconsin, USA).

RNA immunoprecipitation (RIP)

RIP was performed using the Magna RIPTM RNA-binding protein immunoprecipitation kit. Endogenous miR-144-5p binding to GAS5 was pulled down. Cell lysate was incubated in RIP buffer containing magnetic beads coupled with human anti-Ago2 antibody (Millipore). The immunoprecipitated RNA was obtained after the protein was digested with protease K, and the concentration was examined by qRT-PCR.

RNA pull-down

Biotinylated miR-144-5p was labeled with the RNA 3'-End Desthiobiotinylation Kit. Then, RNA pull-down was performed after transfection of biotin-labeled miR-144-5p into HCC cells. Cells were lysed in an RNase-free environment at 4°C. Streptavidin agarose beads (Pierce; Thermo Fisher Scientifi, Inc.) were allowed to react overnight with cell lysate at 4°C to pull down biotin-labeled miRNA and related RNAs. After washing and centrifuging (1,500×g, 10 minutes, 4°C), the precipitate was dissolved with TRIzol®. Then, GAS5 levels in the pull-down sample were quantified by qRT-PCR.

Tumorigenesis in nude mice

Ten BALB/c nude mice (6 weeks, 18-22 g, Vital River, Beijing, China) were reared at 22°C and 50%-70% humidity, with a regular circadian rhythm for adaptive feeding. Hep3B cells stably transfected with sh-NC or sh-GAS5 (1.0×10^5 cells were added to PBS (100 μL) were injected subcutaneously to the right rear paw of male

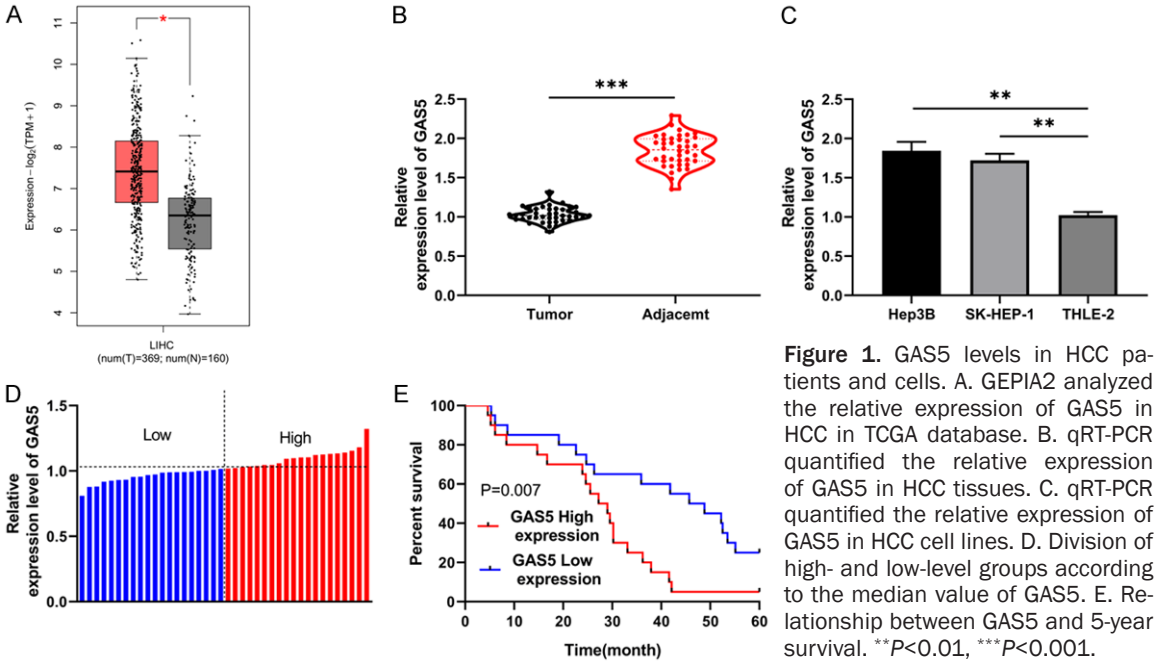

Figure 1. GAS5 levels in HCC patients and cells. A. GEPIA2 analyzed the relative expression of GAS5 in HCC in TCGA database. B. qRT-PCR quantified the relative expression of GAS5 in HCC tissues. C. qRT-PCR quantified the relative expression of GAS5 in HCC cell lines. D. Division of high- and low-level groups according to the median value of GAS5. E. Relationship between GAS5 and 5-year survival. $^{**}P<0.01$, $^{***}P<0.001$.

nude mice (n=5 in each group). When the tumor reached an average volume of approximately 100 mm^3, the mice were exposed to radiation (4 Gy) for 5 days after evaluating the radiosensitivity of HCC *in vivo*. The tumor volume was measured every 7 days. After 35 days, the mice were euthanized and the tumor was weighed.

Statistical analysis

GraphPad 8 was used for graphing and data processing. The data were expressed by mean standard ± deviation (Mean ± SD). Independent samples t-test was used for between-group comparison, one way ANOVA for multiple-group comparison (denoted by F), and LSD-t test for post-hoc pairwise comparison. Repeated measures ANOVA was used for expression analysis at multiple time points (denoted by F), and Bonferroni for post-hoc test. The correlation analysis of genes was performed by Pearson correlation analysis. Patient survival was visualized by K-M curve and compared by the Log-rank test. Statistical significance was set at $P<0.05$.

Results

High levels of GAS5 in HCC decreased the survival of patients

At first, we analyzed GAS5 levels in HCC through GEIPA 2, and TCGA database revealed their elevation in HCC (**Figure 1A**). Also, an elevation of GAS5 levels in 40 patients with HCC was identified by qRT-PCR (**Figure 1B**). Moreover, the cell experiment indicated the increased expression of GAS5 in HCC (**Figure 1C**). After that, we allocated the patients into high- and low-level groups by the median value of GAS5, and analyzed the relationship between GAS5 and patients' survival (**Figure 1D**). It turned out that the 5-year survival in the high level group was lower than that in low level group (**Figure 1D**), suggesting that GAS5 is associated with HCC.

Knocking down GAS5 restricted proliferation and enhances radiosensitivity and apoptosis in HCC

Hep3B and SK-HEP-1 cells were exposed to radiation with graded doses to determine the effect of GAS5 on radiosensitivity of HCC cells. An increase in radiation dose elevated GAS5 levels in cells, showing an increasing trend (**Figure 2A**). In addition, a radiation dose of 6 Gy was used to treat the cells for 24 hours. With an increase of radiation time, GAS5 levels in HCC increased compared with those with a radiation dose of 0 Gy (**Figure 2B**). Therefore, there is an association between GAS5 and radiosensitivity of HCC. Next, we transfected si-GAS5 plasmids into HCC cells, and noticed that si-GAS5#3 had the highest transfection efficiency (**Figure 3A**). To verify whether GAS5 reg-

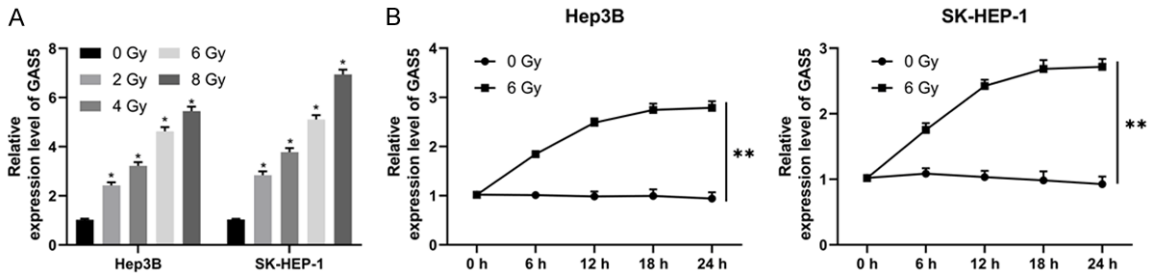

Figure 2. Relationship between GAS5 and radiation doses in HCC cells. A. Changes in relative expression of GAS5 in HCC cells at different radiation doses. B. Changes of relative expression of GAS5 in HCC cells exposed to 6 Gy radiation. $^{*}P<0.05$, $^{**}P<0.01$.

ulates cell sensitivity, HCC cells were treated with si-NC and si-GAS5#3 (**Figure 3B**) and exposed to 6 Gy radiation. Compared with si-NC group, inhibited proliferation was observed in si-GAS5#3 group (MTT assay, **Figure 3C**), as well as reduced colony formation (colony count, **Figure 3D**) and enhanced apoptosis (flow cytometry, **Figure 3E**). In addition, we also found that protein levels of Bax and cle-caspase-3 were increased in si-GAS5#3 group, and those of Bcl-2 were decreased through WB (**Figure 3F**), indicating that knocking down GAS5 induces HCC apoptosis. Overall, knocking down GAS5 hinders proliferation and promotes radiosensitivity and apoptosis in HCC cells.

GAS5 acts as a sponge and regulates miR-144-5p

In order to determine the clinical implication of GAS5, we predicted its possible downstream miRs. It was found that there were potential binding sites between miR-144-5p and GAS5 (**Figure 4A**). Then, RIP RNA pull-down and DLR assay were conducted to verify the binding of GAS5 and miR-144-5p. In RIP, GAS5 and miR-144-5p were precipitated by Ago2 antibody (**Figure 4B**), and RNA pull-down also revealed the interaction between GAS5 and miR-144-5p (**Figure 4C**). In addition, DLR assay revealed the inhibited luciferase activity of GAS5-WT by miR-144-5p-mimics (**Figure 4D**). This suggested that GAS5 can act as a miR-144-5p sponge. Furthermore, according to qRT-PCR, miR-144-5p levels were low in HCC tissues (**Figure 4E**) and reversely correlated with GAS5 (**Figure 4F**). At last, we conducted a co-transfection experiment to verify the regulatory effect of GAS5 on miR-144-5p. Transfection of si-GAS5#3 increased miR-144-5p levels in HCC cells, as shown in qRT-PCR, and inhibited the inhibitory role of anti-miR-144-5p on miR-144-5p (**Figure 4G**). Therefore, GAS5 acts as a sponge and is able to regulate miR-144-5p.

miR-144-5p is able to regulate ATF2

To explore the mechanism of miR-144-5p in regulating radiosensitivity of HCC, we predicted the downstream target genes of miR-144-5p, and ATF2 was found to be a potential target (**Figure 5A**). DLR assay indicated that the luciferase activity of ATF2-WT was inhibited by miR-144-5p-mimics (**Figure 5B**); Moreover, qRT-PCR uncovered high ATF2 levels in HCC (**Figure 5C**), and a reverse association between ATF2 and miR-144-5p and its positive association with GAS5 (**Figure 5D**). These assays suggested that there was a regulatory relation between ATF2 and miR-144-5p. Then, we tried to verify this regulatory relation through co-transfection of cells. ATF2 was upregulated by pcDNA-3.1-ATF2 and was inhibited by co-transfection of miR-144-5p-mimics and pcDNA-3.1-ATF2 (**Figure 5E**). Thus, miR-144-5p is able to regulate ATF2.

GAS5 restricts proliferation and invasion and enhances radiosensitivity of HCC through miR-144-5p/ATF2

We carried out the rescue experiment to confirm the involvement of miR-144-5p/ATF2 axis in the regulation of radiosensitivity of HCC by GAS5. Through co-transfection of anti-miR-144-5p or pcDNA-3.1-ATF2 with si-GAS5#3, we found that si-GAS5#3 restricted the promotion of proliferation and viability in HCC cells which was achieved by anti-miR-144-5p and pcDNA-3.1-ATF2 (**Figure 6A**, **6B**), and reversed the inhibition of apoptosis (**Figure 6C**). Thus,

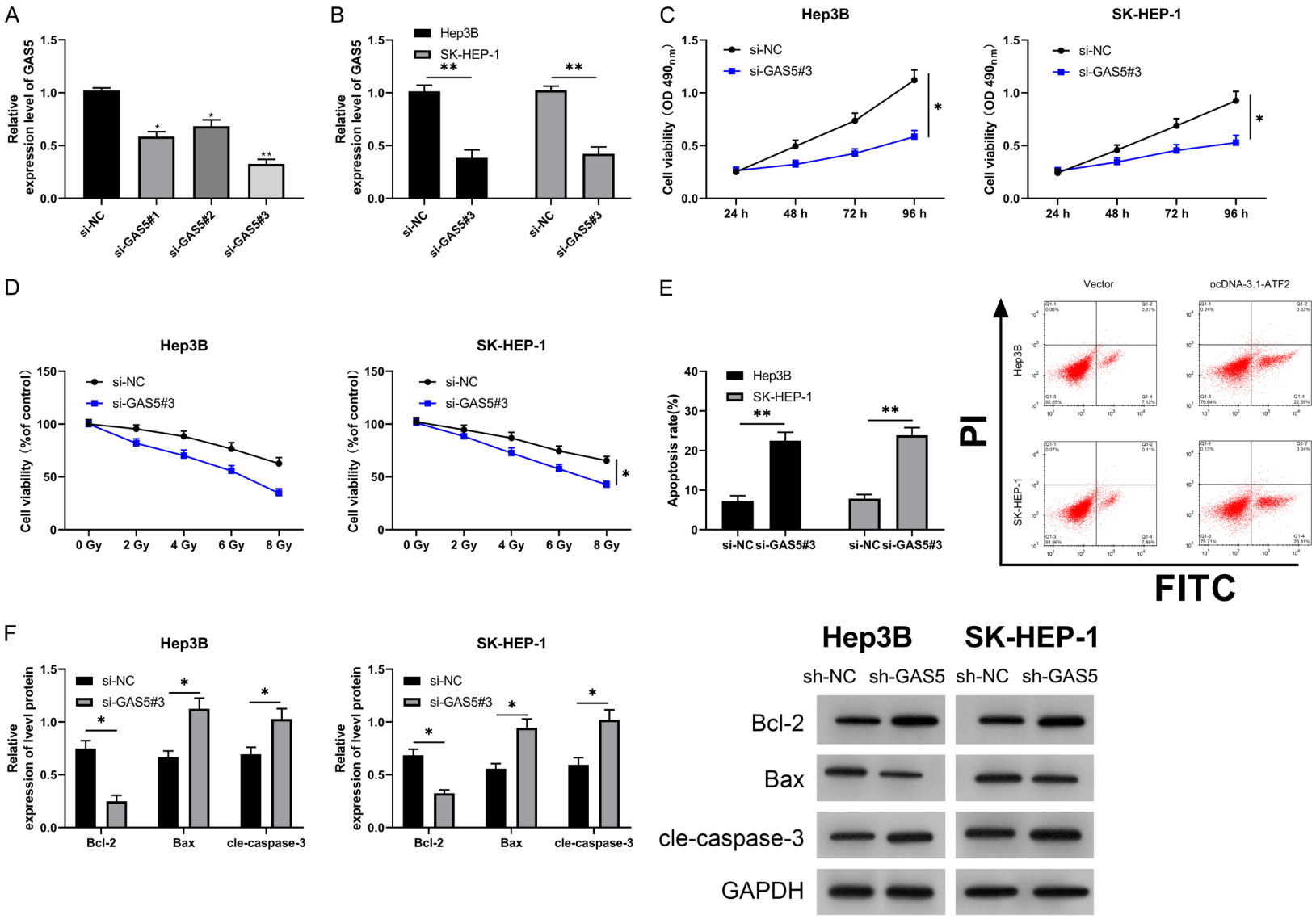

Figure 3. Effect of knocking down GAS5 on radiosensitivity of HCC. A. qRT-PCR determined transfection efficiency of si-GAS5 plasmids. B. qRT-PCR quantified the relative expression of GAS5 in HCC cells transfected with si-GAS5#3. C. MTT assay tested changes in cell proliferation after transfection of si-GAS5#3 under 6 Gy radiation. D. Colony count tested changes in cell viability after transfection of si-GAS5#3 under different doses of radiation. E. Flow cytometry tested changes in cell apoptosis after transfection of si-GAS5#3 under 6 Gy radiation. F. WB tests changed in apoptosis-related proteins after transfection of si-GAS5#3 under 6 Gy radiation. $^{*}P<0.05$, $^{**}P<0.01$.

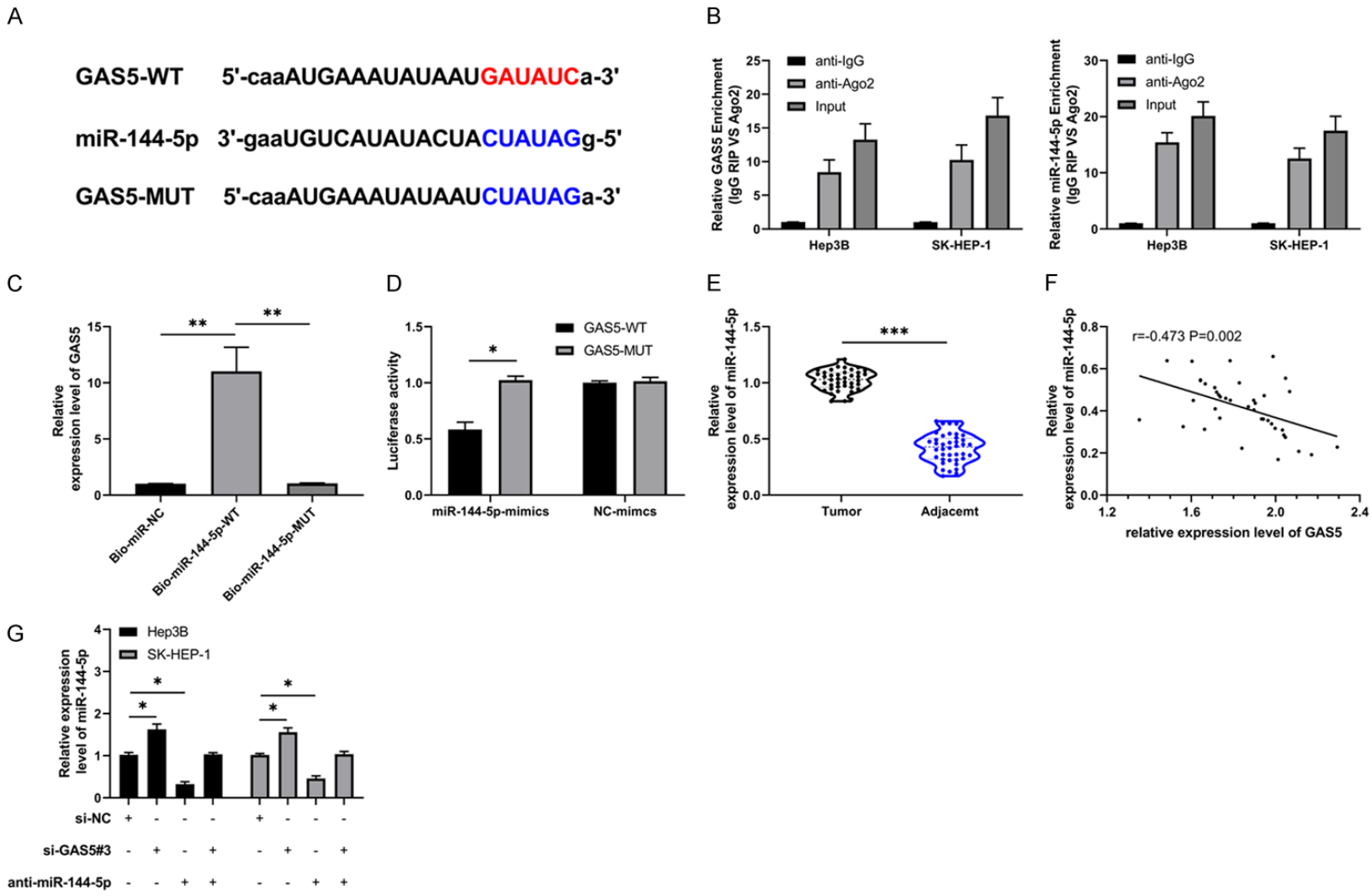

Figure 4. Relationship between GAS5 and miR-144-5p. A. Target binding sites between GAS5 and miR-144-5p. B. GAS5 and miR-144-5p were precipitated by Ago2 antibody (RIP). C. GAS5 interacted with miR-144-5p (RNA pull-down). D. GAS5 interacted with miR-144-5p (DLR assay). E. Relative expression of miR-144-5p in HCC (qRT-PCR). F. Correlation between GAS5 and miR-144-5p (Pearson test). G. Relative expression of miR-144-5p in HCC after co-transfection (qRT-PCR). $^{*}P<0.05$, $^{**}P<0.01$, $^{***}P<0.001$.

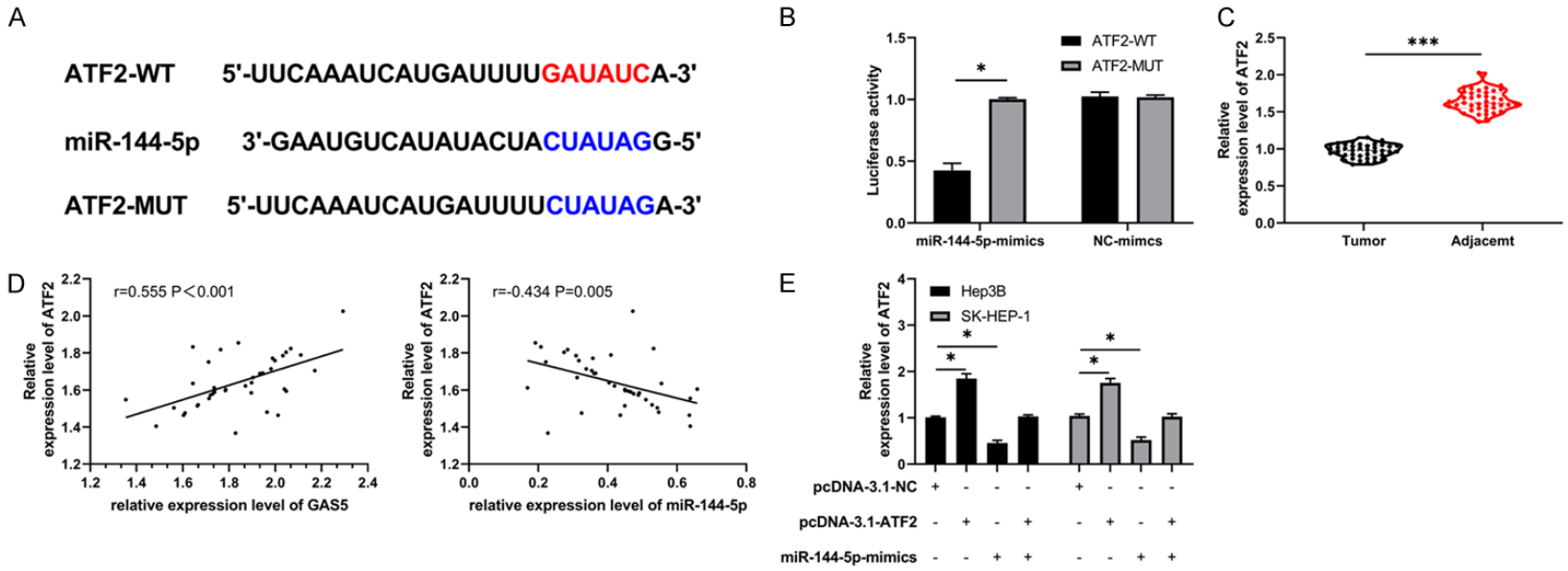

Figure 5. Verification of regulatory relationship between ATF2 and miR-144-5p. A. Target binding sites between miR-144-5p and ATF2. B. miR-144-5p interacted with ATF2 (DLR assay). C. ATF2 levels in HCC tissues (qRT-PCR). D. Correlation between ATF2 and GAS5/miR-144-5p (Pearson test). E. Relative expression of miR-144-5p in HCC after co-transfection (qRT-PCR). $^{*}P<0.05$, $^{***}P<0.001$.

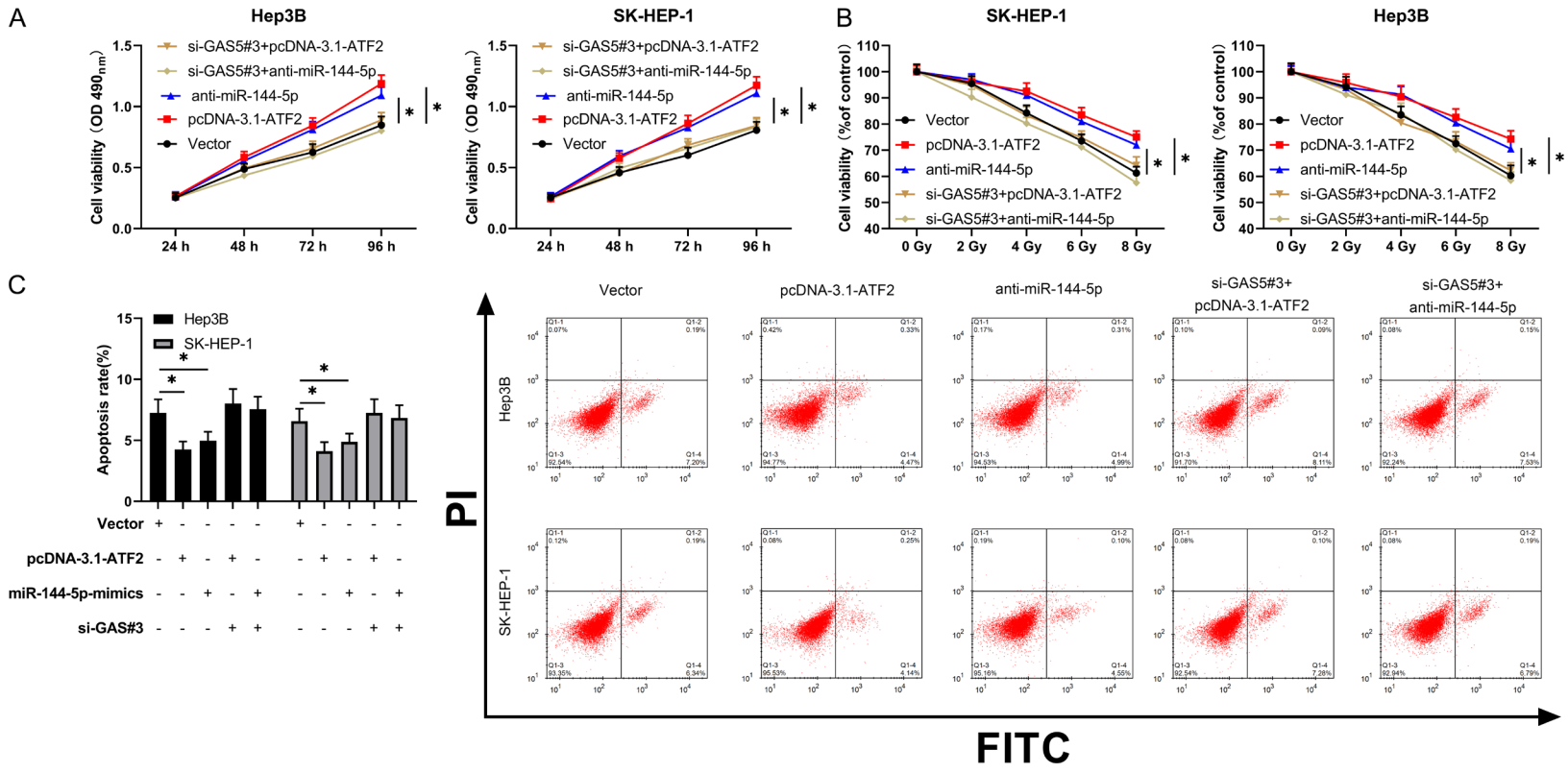

Figure 6. GAS5 restricted proliferation and invasion and enhanced radiosensitivity of HCC via miR-144-5p/ATF2. A. Changes in proliferation in HCC cells after co-transfection (MTT assay). B. Changes in viability in HCC cells after co-transfection (colony count). C. Changes in apoptosis in HCC cells after co-transfection (flow cytometry). *P<0.05.

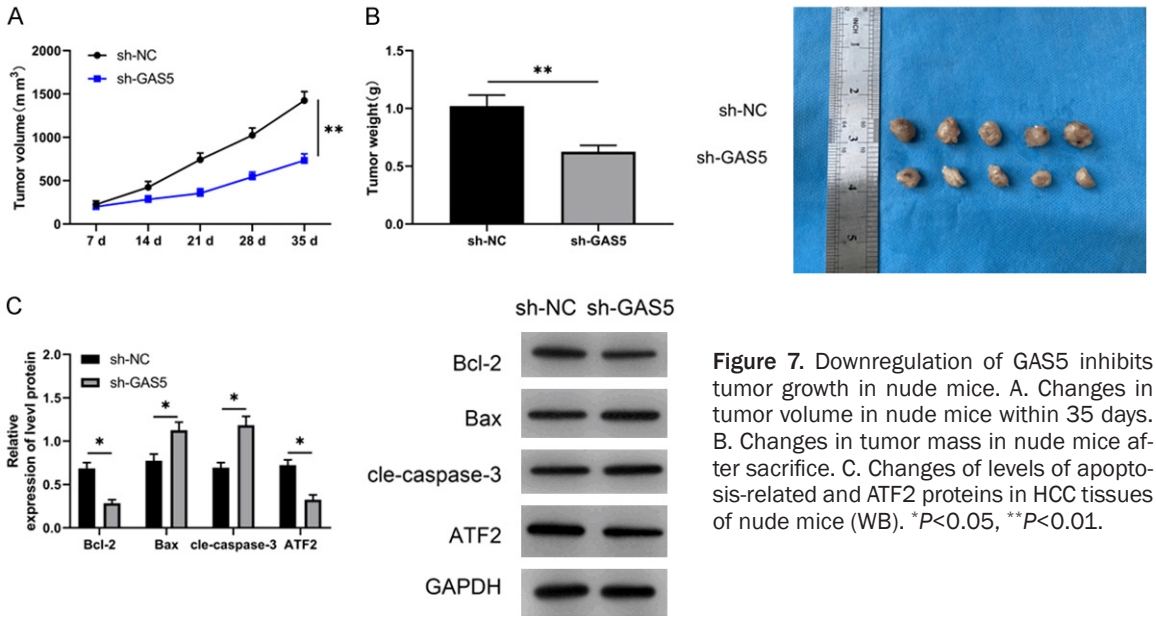

Figure 7. Downregulation of GAS5 inhibits tumor growth in nude mice. A. Changes in tumor volume in nude mice within 35 days. B. Changes in tumor mass in nude mice after sacrifice. C. Changes of levels of apoptosis-related and ATF2 proteins in HCC tissues of nude mice (WB). $^{*}P<0.05$, $^{**}P<0.01$.

GAS5 enhances the radiosensitivity of HCC via miR-144-5p/ATF2 axis.

Downregulation of GAS5 inhibits tumor growth in nude mice

Tumor growth in nude mice injected with lentivirus sh-GAS5 and sh-NC plasmids were monitored to estimate the anti-tumor effect of GAS5 *in vivo*. It turned out that the tumor volume in sh-GAS5 group was lower than that in sh-NC group (**Figure 7A**), and the mass was also reduced (**Figure 7B**). Tumor tissues were collected after the sacrifice of nude mice. Protein levels of ATF2 and Bcl-2 in sh-GAS5 group were lower, and those of Bax and cle-caspase-3 were higher than those in sh-NC group (**Figure 7C**), suggesting that GAS5 enhances the radiosensitivity of HCC.

Discussion

Despite considerable progress in the treatment of HCC, drug and radiation resistance has remained a thorny problem [22]. In the present study, increased GAS5 was observed in HCC, and its inhibition enhanced the radiosensitivity, which is expected to be a therapeutic target.

LncRNAs have been widely reported to regulate cell growth and metastasis in a variety of cancers [23, 24], and enhance their radiosensitivity. Xiu et al. believe that knocking down lncRNA TUG1 enhances the radiosensitivity of prostate cancer through TUG1/miR-139-5p/SMC1A axis [25]. GAS5, an regulator of tumor radiosensitivity, is associated with radiosensitization of prostate cancer [26] and non-small cell lung cancer [27]. GAS5 contributes to the increase in cisplatin sensitivity in HCC [17], but the effect of GAS5 on radiosensitivity of HCC has never been dissected. Increased levels of GAS5 in HCC were identified, resulting in decreased 5-year survival, which was consistent with previous findings. We also noticed that the radiosensitivity of HCC increased after knocking down GAS5, and then induced apoptosis.

ceRNAs have been mentioned frequently in recent studies, and lncRNAs are capable of acting as miR sponges to regulate genes and participate in cancer progression [28]. For instance, lncRNA SNHG1 acts as a molecular sponge to mediate miR-195, thereby promoting cell proliferation and invasion in HCC [29]. In the present study, target binding sites between GAS5 and miR-144-5p were found through an online tool, and GAS5 was able to regulate miR-144-5p levels. Therefore, we have confirmed that GAS5 can act as a sponge for miR-144-5p, suggesting that miR-144-5p is driven by GAS5 to participate in radiosensitivity of HCC.

ATF2 is a member of the leucine zipper family of DNA binding proteins that participates in DNA-damage response in cells [30]. Also, ATF2

shares target binding sites with miR-144-5p, and has an inhibitory effect on radiosensitivity of lung cancer [31]. A series of measurements implemented in this study demonstrated that ATF2 presented high levels in HCC tissues, and bound to miR-144-5p. In addition, miR-144-5p-mimics effectively inhibited the overexpression of ATF2 induced by pcDNA-3.1-ATF2 in HCC. So, we speculated that there was a axial relationship in GAS5/miR-144-5p/ATF2. To verify this, we carried out a rescue experiment, and found that si-GAS5#3 remarkably inhibited the promoting effect of anti-miR-144-5p and pcDNA-3.1-ATF2 on proliferation and viability, and their inhibitory effect on apoptosis. In addition, knocking out GAS5 inhibited the protein levels of ATF2 and induced apoptosis *in vitro*.

However, there are several limitations. The invasion and migration in cells transfected with si-GAS5 were not analyzed. Moreover, whether GAS5/miR-144-5p/ATF2 pathway can enhance cisplatin sensitivity of HCC cells remains unknown. We will conduct more experiments to address these limitations and enrich our results.

To sum up, overexpression of GAS5 upregulates ATF2 through miR-144-5p and is able to enhance the radiosensitivity of HCC.

Disclosure of conflict of interest

None.

Address correspondence to: Qinghuan Li, Oncology Radiotherapy Center, Xiangyang Central Hospital, Affiliated Hospital of Hubei University of Arts and Science, Funiu Road, Xiangzhou District, Xiangyang 441021, Hubei, China. Tel: +86-13581426174; E-mail: qinghuanli1001@163.com

References

[1] Hartke J, Johnson M and Ghabril M. The diagnosis and treatment of hepatocellular carcinoma. Semin Diagn Pathol 2017; 34: 153-159.

[2] Bray F, Ferlay J, Soerjomataram I, Siegel RL, Torre LA and Jemal A. Global cancer statistics 2018: GLOBOCAN estimates of incidence and mortality worldwide for 36 cancers in 185 countries. CA Cancer J Clin 2018; 68: 394-424.

[3] Franco RA, Fan Y, Jarosek S, Bae S and Galbraith J. Racial and geographic disparities in hepatocellular carcinoma outcomes. Am J Prev Med 2018; 55 Suppl 1: S40-S48.

[4] Hung GY, Horng JL, Yen HJ, Lee CY and Lin LY. Changing incidence patterns of hepatocellular carcinoma among age groups in Taiwan. J Hepatol 2015; 63: 1390-1396.

[5] Fujiwara N, Friedman SL, Goossens N and Hoshida Y. Risk factors and prevention of hepatocellular carcinoma in the era of precision medicine. J Hepatol 2018; 68: 526-549.

[6] Budny A, Kozlowski P, Kaminska M, Jankiewicz M, Kolak A, Budny B, Budny W, Niemunis-Sawicka J, Szczypior G, Kurniawka B and Burdan F. Epidemiology and risk factors of hepatocellular carcinoma. Pol Merkur Lekarski 2017; 43: 133-139.

[7] Lurje I, Czigany Z, Bednarsch J, Roderburg C, Isfort P, Neumann UP and Lurje G. Treatment strategies for hepatocellular carcinoma (-) a multidisciplinary approach. Int J Mol Sci 2019; 20: 1465.

[8] Yu Y and Feng M. Radiotherapy for hepatocellular carcinoma. Semin Radiat Oncol 2018; 28: 277-287.

[9] Meyer J and Singal AG. Stereotactic ablative radiotherapy for hepatocellular carcinoma: history, current status, and opportunities. Liver Transpl 2018; 24: 420-427.

[10] Kalogeridi MA, Zygogianni A, Kyrgias G, Kouvaris J, Chatziioannou S, Kelekis N and Kouloulias V. Role of radiotherapy in the management of hepatocellular carcinoma: a systematic review. World J Hepatol 2015; 7: 101-112.

[11] Ferre F, Colantoni A and Helmer-Citterich M. Revealing protein-lncRNA interaction. Brief Bioinform 2016; 17: 106-116.

[12] Li J, Meng H, Bai Y and Wang K. Regulation of lncRNA and its role in cancer metastasis. Oncol Res 2016; 23: 205-217.

[13] Zhang Y, Xu Y, Feng L, Li F, Sun Z, Wu T, Shi X, Li J and Li X. Comprehensive characterization of lncRNA-mRNA related ceRNA network across 12 major cancers. Oncotarget 2016; 7: 64148-64167.

[14] Shi R, Wu P, Liu M, Chen B and Cong L. Knockdown of lncRNA PCAT6 enhances radiosensitivity in triple-negative breast cancer cells by regulating miR-185-5p/TPD52 axis. Onco Targets Ther 2020; 13: 3025-3037.

[15] Li J, Yang C, Li Y, Chen A, Li L and You Z. LncRNA GAS5 suppresses ovarian cancer by inducing inflammasome formation. Biosci Rep 2018; 38: BSR20171150.

[16] Esguerra JLS, Ofori JK, Nagao M, Shuto Y, Karagiannopoulos A, Fadista J, Sugihara H, Groop L and Eliasson L. Glucocorticoid induces human beta cell dysfunction by involving riborepressor GAS5 LincRNA. Mol Metab 2020; 32: 160-167.

[17] Zhao P, Cui X, Zhao L, Liu L and Wang D. Overexpression of growth-arrest-specific transcript

5 improved cisplatin sensitivity in hepatocellular carcinoma through sponging miR-222. DNA Cell Biol 2020; 39: 724-732.
[18] Issue information-declaration of Helsinki. J Bone Miner Res 2018; 33: BM i-BM ii.
[19] Livak KJ and Schmittgen TD. Analysis of relative gene expression data using real-time quantitative PCR and the 2(-delta delta C(T)) method. Methods 2001; 25: 402-408.
[20] Paraskevopoulou MD, Vlachos IS, Karagkouni D, Georgakilas G, Kanellos I, Vergoulis T, Zagganas K, Tsanakas P, Floros E, Dalamagas T and Hatzigeorgiou AG. DIANA-LncBase v2: indexing microRNA targets on non-coding transcripts. Nucleic Acids Res 2016; 44: D231-D238.
[21] Li JH, Liu S, Zhou H, Qu LH and Yang JH. starBase v2.0: decoding miRNA-ceRNA, miRNA-ncRNA and protein-RNA interaction networks from large-scale CLIP-Seq data. Nucleic Acids Res 2014; 42: D92-97.
[22] Schaub SK, Hartvigson PE, Lock MI, Hoyer M, Brunner TB, Cardenes HR, Dawson LA, Kim EY, Mayr NA, Lo SS and Apisarnthanarax S. Stereotactic body radiation therapy for hepatocellular carcinoma: current trends and controversies. Technol Cancer Res Treat 2018; 17: 1533033818790217.
[23] Zhou F, Shen F, Zheng Z and Ruan J. The LncRNA XIRP2-AS1 predicts favorable prognosis in colon cancer. Onco Targets Ther 2019; 12: 5767-5778.
[24] Li C, Lei Z, Peng B, Zhu J and Chen L. LncRNA HCP5 stimulates the proliferation of non-small cell lung cancer cells by up-regulating survivin through the down-regulation of miR-320. Cancer Manag Res 2020; 12: 1129-1134.
[25] Ren Y, Shang J, Li J, Liu W, Zhang Z, Yuan J and Yang M. The long noncoding RNA PCAT-1 links the microRNA miR-215 to oncogene CRKL-mediated signaling in hepatocellular carcinoma. J Biol Chem 2017; 292: 17939-17949.
[26] Yang J, Hao T, Sun J, Wei P and Zhang H. Long noncoding RNA GAS5 modulates alpha-Solanine-induced radiosensitivity by negatively regulating miR-18a in human prostate cancer cells. Biomed Pharmacother 2019; 112: 108656.
[27] Xue Y, Ni T, Jiang Y and Li Y. Long noncoding RNA GAS5 inhibits tumorigenesis and enhances radiosensitivity by suppressing miR-135b expression in non-small cell lung cancer. Oncol Res 2017; 25: 1305-1316.
[28] Karreth FA and Pandolfi PP. ceRNA cross-talk in cancer: when ce-bling rivalries go awry. Cancer Discov 2013; 3: 1113-1121.
[29] Zhang S and Song X. Long non-coding RNA SNHG1 promotes cell proliferation and invasion of hepatocellular carcinoma by acting as a molecular sponge to modulate miR-195. Arch Med Sci 2020; 16: 386-394.
[30] Watson G, Ronai ZA and Lau E. ATF2, a paradigm of the multifaceted regulation of transcription factors in biology and disease. Pharmacol Res 2017; 119: 347-357.
[31] Song L, Peng L, Hua S, Li X, Ma L, Jie J, Chen D, Wang Y and Li D. miR-144-5p enhances the radiosensitivity of non-small-cell lung cancer cells via targeting ATF2. Biomed Res Int 2018; 2018: 5109497.